



Behavior of Self Compacted Concrete Ferrocement Beams

Abeer M. Erfan ^{a*}, Tamer H. K. Elafandy ^b, Mahmoud M. Mahran ^a
and Mohamed Said ^a

^a Department of Civil Engineering, Shoobra Faculty of Engineering/ Beniha University, 108 Shoobra St., Shoobra, Cairo, Egypt.

^b Department of Civil Engineering, Housing and Building Research Center (HBRC), Cairo, Egypt.

Authors' contributions

This work was carried out in collaboration among all authors. All authors read and approved the final manuscript.

Article Information

DOI: 10.9734/JERR/2021/v21i117434

Editor(s):

- (1) Prof. Hamdy Mohy El-Din Afefy, Pharos University, Egypt.
- (2) Dr. P. Elangovan, SRM TRP Engineering College, India.

Reviewers:

- (1) APACO JOAN, Kyambogo University, Uganda.
- (2) Godwin Anwara Ibe, Akanu Ibiam Federal Polytechnic, Nigeria.
- (3) Tayyab Naqash, Islamic University Madinah, Saudi Arabia.
- (4) Qasim M. Shakir, University of Kufa, Iraq.

Complete Peer review History: <https://www.sdiarticle4.com/review-history/73935>

Original Research Article

Received 14 July 2021
Accepted 24 September 2021
Published 29 September 2021

ABSTRACT

This study presents the results of an experimental investigation into the behaviour of ferrocement beams after exposure to various types of ferrocement and ferrocement layers. In the experimental programme, seven simply supported beams were tested up to failure under a four-point load. The dimensions of all specimens are 15cm×25cm×200cm. Each beam was reinforced using steel 2φ12 on bottom and 2φ10 on the top and therefore the stirrups were 10 φ 10/m. Six beams were also strengthened with ferrocement layers and varied steel wire meshes. The test specimens are divided into three groups, and the results of each group are compared to those of the control specimen. The first group (A) used the welded wire mesh. The second group (B) used the expanded wire mesh. However, the third group (C) used woven wire mesh. The tested beams' mid-span cracks, deflection, concrete strains, and reinforcement were all measured and compared. The test beams' efficiency was evaluated in terms of energy absorption and ultimate flexure load cracking behaviour. The experimental results emphasize that high ultimate loads, better crack resistance control, high ductility, and good energy absorption properties could be achieved using the proposed ferrocement beams. The use of woven, expanded, and welded wire mesh reduced

crack propagation and reduced the number and width of cracks, especially in specimens with two layers of wire mesh. Theoretical calculations were carried out in order to compare the obtained results to the theoretical ones, which were found to be in good agreement.

Keywords: Ferrocement beams; RC beams; steel mesh; ultimate load; cracking.

1. INTRODUCTION

Ferrocement has a higher tensile strength to weight ratio and better cracking resistance behavior when compared to reinforced concrete. As a result, it has been extensively used to construct different element such as, tanks, roofs..etc. Subsidence of reinforced concrete structures has become more common in recent decades as a result of higher service loads and/or durability issues. economic losses due to such failures are billions of dollars. Mansur [1] In 1990, ferrocement rect.-section short columns with concrete infill were subjected to eccentric and axial compression in an experimental study. The kinds, configurations, and volume fraction of reinforcement were the study's main parameters. A ferrocement box-section can be employed as a structural beam, according to test results. Welded wire mesh has been found to perform better than an equivalent amount of woven mesh. In 2013, Khan et al. [2] beams having a concrete section of 150x200mm and length of 1800mm with different numbers and layers of ferrocement were cast. All beams were tested with 1650 mm test spans and constant shear span to depth beams under two-point stress until the service limit. Only the dominating zone of failure has been reinforced, and the beams have been tested until they fail the same under the load pattern. The most effective approach has been determined to be fortified by a layer of cast-in-place ferro-mesh, while the strengthened of the beams through the use of a precast ferrocement layer is not only simple to do at home, it also has the potential to improve load carrying capacity, stiffness, and ductility. Another interesting research work was done by Rashid in 2016 et al. [3] revealed that from the analyses the load-deflection relationships until failure modes, crack patterns and failure modes were obtained. The ultimate shear load carrying capacity of the beams retrofitted with a 12mm layer of ferrocement rose 16.67% when compared to the control beam, according to the results. Aqeel et al. [4] the first cracking and ultimate loads increased as the wire mesh layers in web and bottom flange increased, With increased mortar compressive strength and

wire mesh layers in the web and bottom flange, the deflection of the tested beams reduced. Within 9%, the finite element model and the experimental data accord well. In 2009, Hazem [5] looked at the usage of U-section ferrocement permanent forms for beam building, while Abdel Tawab [6] explored the use of U-shaped ferrocement permanent forms for the construction of beams in 2006. A short programme was created to gather information on the effects of ferrocement repair on short columns subjected to axial loads. In 2014, Nagan [7] published a paper on the impact resistance of geopolymer mortar slabs. For this, specimens of size 23x23x2.5cm as shown Fig. 2 with four layers of chicken mesh two layers of rectangular weld mesh and a combination of for impact loading, a single layer of weld mesh and four layers of chicken mesh were cast and dropped weight tested. When adding top mesh steel to ferrocement geopolymer raised the impact residual strength ratio by 4-28 compared to a plain ferrocement mortar slab. Abdel in 2012 et al. [8] Properties have great strength, crack resistance, and energy absorption when compared to conventional reinforced concrete beams of the same size and total reinforcing steel content, regardless of the kind of steel mesh and number of layers in the ferrocement laminate. SCC is a type of concrete that can fill a mould with minimal defects and compacts without vibrating under its own weight. The resulting concrete is more cohesive, flows without segregation or bleeding, and has a higher quality Muna 2016 [9]. Self-compacting concrete (SCC) is a preferred substitution for conventional concrete where highly congested reinforcement is present or forms with complex shapes need to be filled. It has the capacity to flow and consolidate under its own weight without the need for mechanical vibration (ACI 237R-07) [10]. Although a lack of manuals and codes has hindered SCC's widespread use, it is predicted to grow in popularity as a cost-cutting choice around the world. A more than important research on the structural shear behaviour and efficiency of R.C structures constructed with SCC have been published [11-15].

2. EXPERIMENTAL PROGRAM

The experimental program consisted of seven composite beam section having the dimensions of 150 mm width, 250 mm depth, and 2000 mm length of span were cast and tested up to failure under four-point load. All specimens were reinforced using steel 2 ϕ 12 on bottom and 2 ϕ 10 on the top and 10 ϕ 10/m for stirrups. Six beams were also strengthened with ferrocement layers and varied steel wire meshes as (welded, expanded and woven)

2.1 Characteristics of Materials

Table 1 show the concrete mixture for the experimental program which gives concrete characteristic strength of 30 MPa. The yield strength was 360 MPa. The characteristics of used composite layers either expanded, welded and woven wire meshes were summarized in Table 2 and shown in Fig.1.

Table 1. Concrete Mixes, Materials Weights

Materials	Mix components $F_{cu} = 30 \text{ MPa}$
Silica fume	55 kg/m ³
Cement	550 Kg/m ³
Coarse aggregate	810 Kg/m ³
Fine aggregate	900 Kg/m ³
Water	200 L/m ³
Super-plasticizer	6.5 L/m ³








2.2 Preparation of Specimens and Samples Description

The experimental program consists of seven beams the first beam is control beam B01, having the same geometry and steel reinforcement details as shown in Figure 1. The control specimen is a rectangular section beam reinforced using 2 ϕ 10 on top and 2 ϕ 12 on bottom and 10 ϕ 10/m as stirrups along the span of tested specimens. Group A consists of two beams B02 and B03 which are reinforced using one, two layers of welded wire mesh respectively. The group B for specimens B04 and B05 which reinforced using one, two layers of expanded wire meshes instead of stirrups respectively as described in Table 2. For group C of B06 and B07 which used one, two layers of woven wire meshes described in Table 2. The mechanical properties of the ferrocement composites are given in Table 3 and the type of ferrocement in Fig. 2.

2.3 Test Setup

The tested beam sections were tested under a four-point load testing machine of the maximum capacity of 600 KN with 1800 mm effective span and 100 mm distance between two loads as shown in Fig.3. The load was effective at 20 KN increments on the tested specimens. The LVDT and dial gages were used with high accuracy to measure the deflections and strains for steel and concrete. The load was kept increasing until the failure load and maximum displacements were reached.

Table 2. Specimens Descriptions and Notations

Group	Specimen ID.	Description of specimens	Reinforcement		Reinforcement configuration
			tension	Comp.	
Control	B01	Control specimen	2 ϕ 12	2 ϕ 10	
A	B02	One layer welded wire mesh	2 ϕ 12	2 ϕ 10	
	B03	Two layer welded wire mesh	2 ϕ 12	2 ϕ 10	
B	B04	One layer expanded wire mesh	2 ϕ 12	2 ϕ 10	
	B05	Two layer expanded wire mesh	2 ϕ 12	2 ϕ 10	
C	B06	One layer woven wire mesh	2 ϕ 12	2 ϕ 10	
	B07	Two layer woven wire mesh	2 ϕ 12	2 ϕ 10	

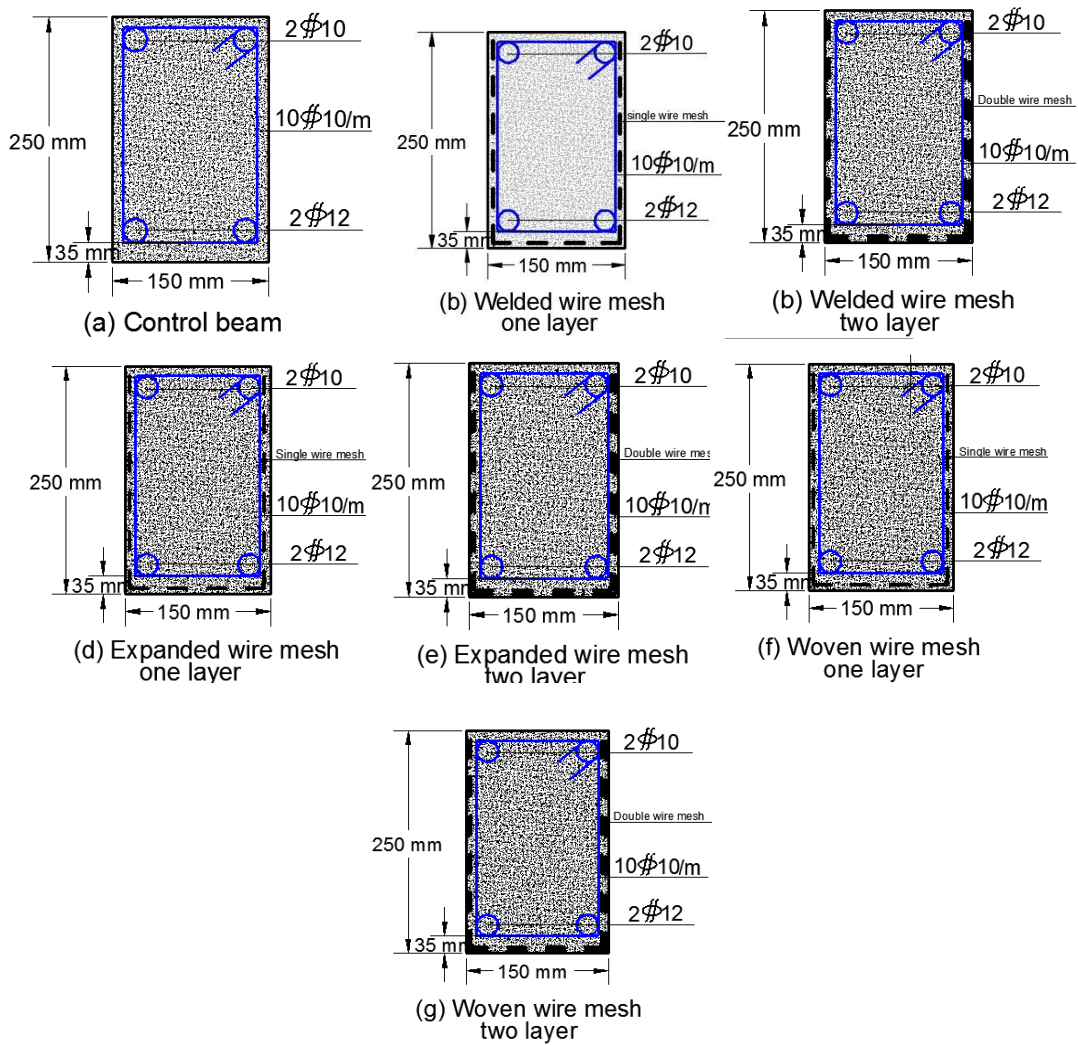
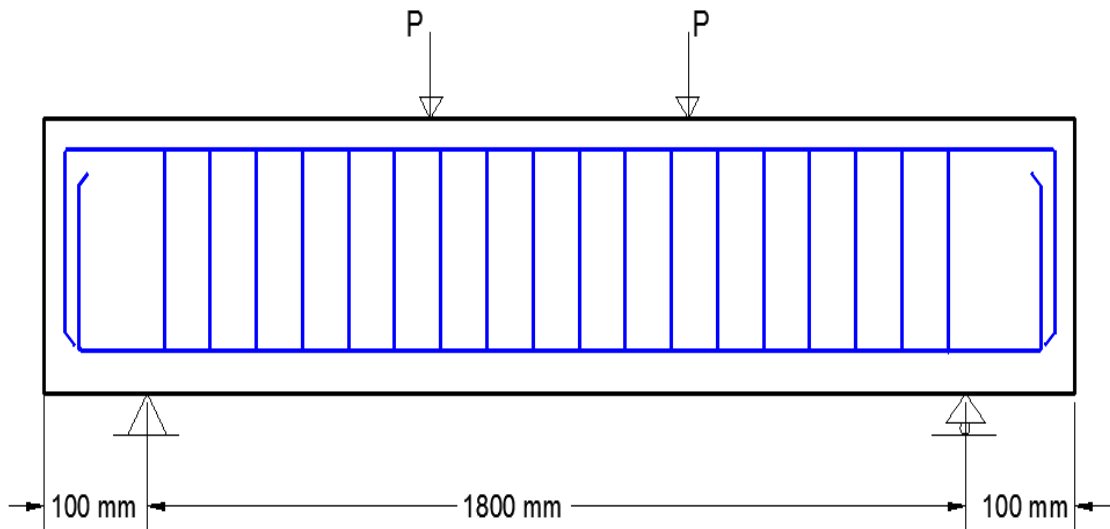
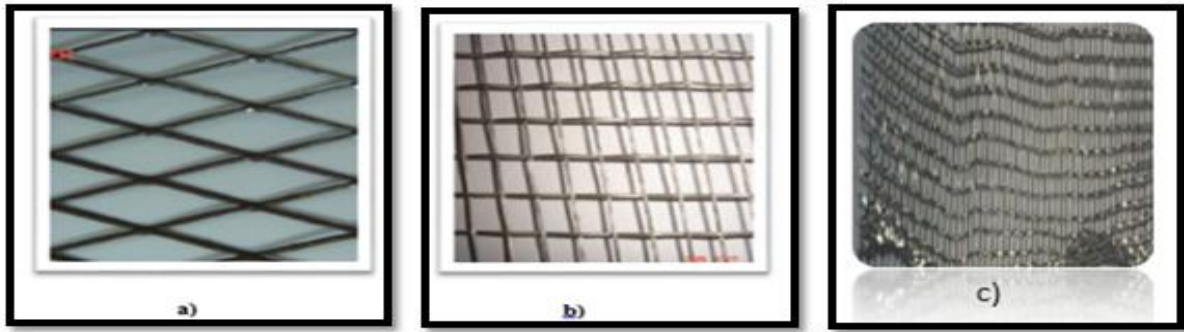


Fig. 1. Beams geometric shape and reinforcement details

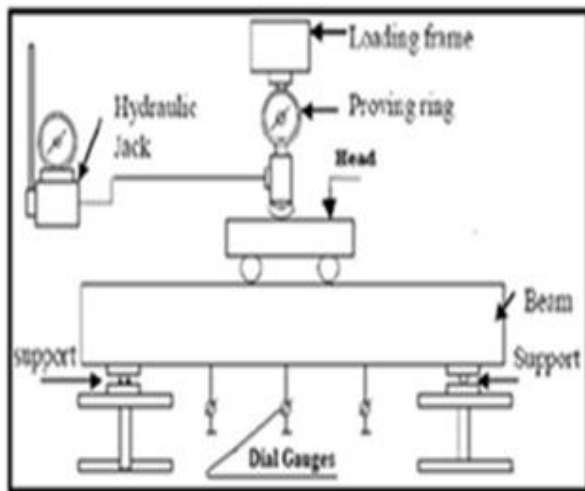


a) Expanded wire mesh, b) welded wire mesh; c) Woven wire mesh.

Fig. 2. Ferrocement Meshes

Table 3. Mechanical properties of expanded,welded , and woven wire meshes

Mesh type	Tensile strength (MPa)	Young's modulus (MPa)	Opens dimensions (mm)	Diameter (mm)
welded wire mesh	400	1700	10.0x10.0	0.7
Expanded wire mesh	250	1200	31.0x16.5	1.25
woven wire mesh	600	1500	4.0x4.0	2.0



a)

a) schematic shape



b)

b) photo the test set up

Fig. 3. Test Set up

3. TEST RESULTS AND DISCUSSION

The cracks propagation during the tests was recorded. The crack initialization in the specimens reinforced using wire meshes was developed, however at later stages with respect to the control specimen. Besides, the crack's lengths and widths decreased in the specimens

reinforced with either welded, expanded, or woven wire meshes as compared to the control specimen.

3.1 Ultimate Failure Load and Deflection

Table 4 and Fig. 4, 5 show the experimental failure loads and related deflections for the

control beam B01. At the half-span, the deflection was measured using an LVDT in comparison to the appropriate experimental loads. It was observed that the load-deflection curves for specimens reinforced using ferrocement composites were semi bilinear especially after reaching failure load, which decreased very rapidly. This behavior was due to the failure mechanism of ferrocement and the type of concrete. For B01, the ultimate failure load was 64.0 KN with a deflection of 47.0 mm.

For group A which has concrete strength equal to 30 MPa and reinforcing using one layer and two layers of welded wire mesh of B02 and B03 respectively, the failure loads were 68.5 KN and 85.6 KN respectively. The deflections were 32.0 mm and 20.4 mm, the deflection decreased and the failure load increased due to the high tensile strength of ferrocement layers composites with enhancement ratios of 31.6% and 56.6% for B02 and B03 respectively as given in Table 4.

For group B which used expanded wire meshes, recorded failure loads of 64.31 KN and 71.0 KN for B04 and B05 respectively. The deflection of B04 was 30.0 mm but was 22.3 mm for B05 which used two layers of expanded wire meshes with enhancement ratios of 36.1% and 52.3% for B04 and B05 respectively as given in Table 4.

For group, C used woven wire mesh of high tensile strength and opens spaces concerning the other wire meshes B06 and B07. The experimental failure loads were 78.5 KN and 89.0 KN respectively verse 24.4 mm and 20.3 mm in deflection. This type of composite wire meshes shows the most enhancement ratios in failure load capacity and deflection to be 22.6% and 39.1% in carrying load capacity and 48.1% and 57.1% in deflections. These results indicate the good effect of using this type of ferrocement composites in ultimate carrying capacity and deflection as in Fig. 6.

3.2 Mode of Failure

This mode of failure was different for flexural failures, especially for beams reinforced with B01 steel bars. For specimens B02 to B07, the failure was tensile failure, which refers to the failure mechanism of ferrocement composites. This was as the previous study [4,5] recorded a similar mode of failure in specimens reinforced by ferrocement composites. Near failure, the control specimen failed in a mode of tension failure accompanied by local crushing and spalling of the concrete on the surface of the beams. For the other series of the tested specimens, near failure, the load reaches the maximum value, and after this value the load-decreased up to 70% to 50% of the maximum load with increasing the descending part of load displacement curves as shown in Table 5.

3.3 Volume Fraction of Steel Reinforcement

Experimental results revealed that increasing the volume fraction of steel reinforcement contributed to a relatively higher ultimate load. This is clear when comparing beam B01 and the other beams which show the different degrees of increase the ultimate failure load, and enhance many properties.

3.4 Ductility and Energy Absorption

Table 5 Shows the energy absorption and the ductility ratio for all tested beams. A progressive increase energy absorption with volume fraction percentage and ductility was observed. For the control specimen, the energy absorption was recorded to be 1504.0 KN.mm. Comparing this value with the recorded values for different groups showed a large increase in the energy absorption capacity for all specimens.

Table 4. Comparison Between Failure Loads of Test Specimens

Group	Specimen ID.	Failure load (KN)	Ultimate deflection (mm)	% of enhancement $\left(\frac{Pu - Pu_{control}}{Pu_{control}}\right)$	% of deflection enhancement $\left(\frac{\Delta u - \Delta u_{control}}{\Delta u_{control}}\right)$
Control	B01	64.0	47.0	-----	-----
A	B02	68.5	32.0	7.03	31.9
	B03	85.6	20.4	33.75	56.6
B	B04	64.3	30.0	0.47	36.1
	B05	71.0	22.3	11.09	52.3
C	B06	78.5	24.4	22.6	48.1
	B07	89.0	20.3	39.10	57.1

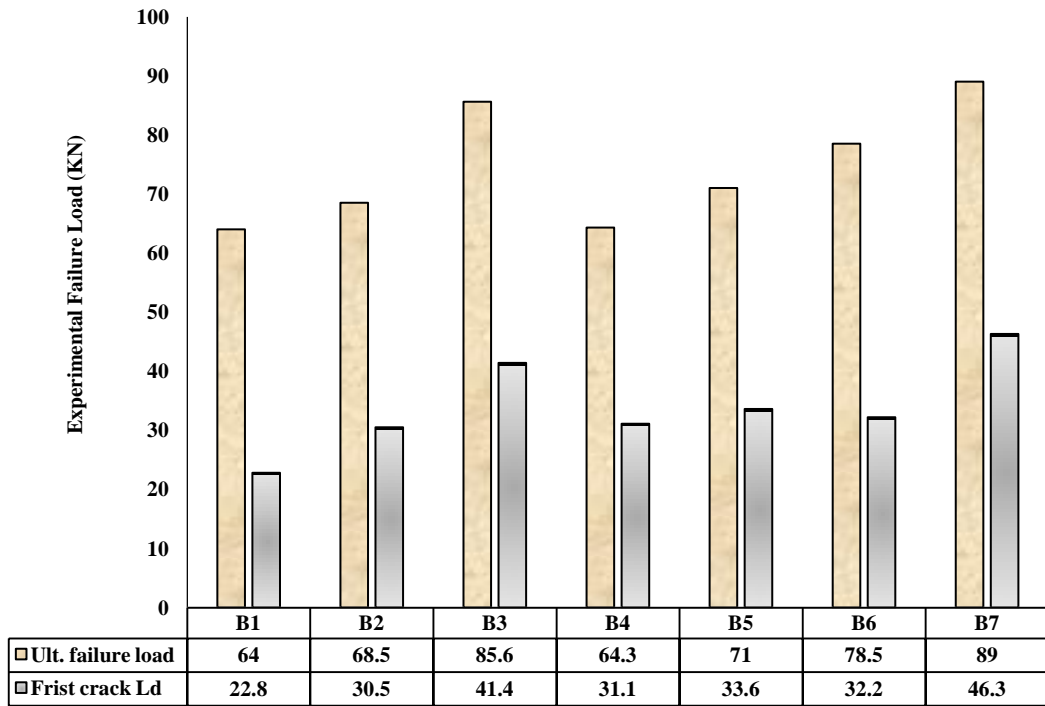


Fig. 4. Comparisons between Ultimate Failure Load and First Crack Load

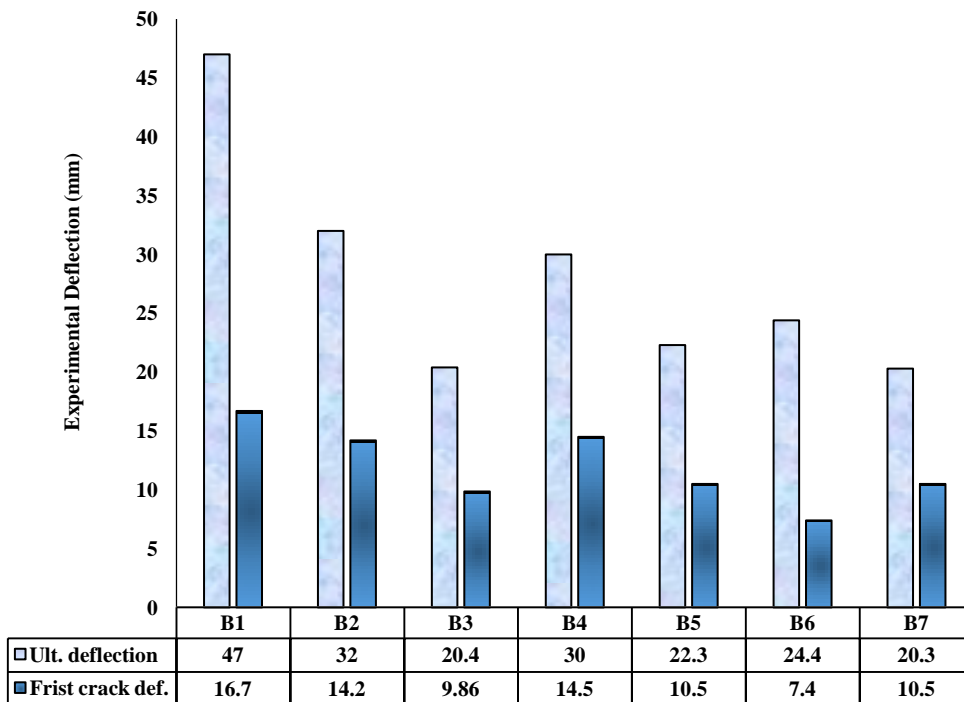


Fig. 5. Comparisons between Ultimate Deflection and First Crack Load

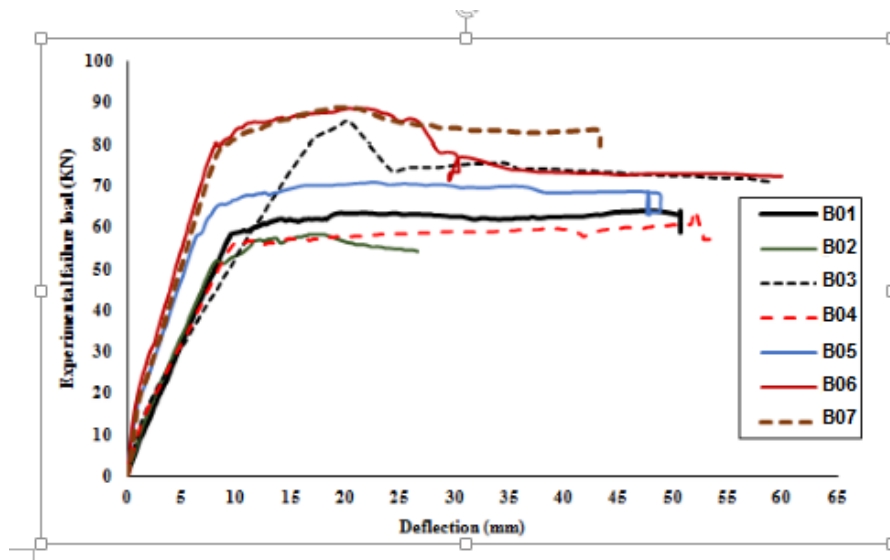


Fig. 6. Load Deflection curves of The Tested Beams

Table 5. Comparison Between Experimental Results

Group	Specimen ID.	Frist crack load (KN)	Ultimate Failure load (KN)	Ductility (%)	Energy absorption (KN.mm)
Control	B01	22.8	64.0	35.6	1504.0
A	B02	30.5	68.5	44.5	1096
	B03	41.4	85.6	48.4	873.12
B	B04	31.1	64.3	48.3	964.5
	B05	33.6	71.0	47.3	791.65
C	B06	32.2	88.5	36.4	902.7
	B07	46.3	89.0	52.0	903.7

The ductility ratio was obtained for the control specimen was 36.6 %. A progressive increase in ductility was obtained for different groups of specimens. For series A, the ductility varied between 44.5 % and 48.4% for B02 and B03. For series B and C, the ductility varied between 36.0% to 52.0%. This shows the enhancement in ductility in beams using ferrocement layers.

Finally, the behaviour of the tested beams was improved by using these innovative composite materials. It can be stated that it delayed the appearance of the first cracks and increased the service load capacity. In addition, it developed high ultimate loads, crack resistance, better deformation characteristics, high durability, high ductility, and energy absorption properties, which are very useful for dynamic applications.

3.5 Cracking Propagation

The control specimen B01 the first crack in this specimen started at the load of 23.6 KN developed under the load point in the mid-span as shown in Fig. 5 and Table 5.

Specimen B02 & B03 the recorded first crack load noticed was 30.4 KN and 41.4 KN for B02 and B03 respectively. This showed an enhancement of about 33.7% and 81.6% respectively

For specimen B04 & B05 which reinforced using 2φ12 as tension steel and 2φ10 as compression steel without stirrups. The one layer and two layers expanded wire meshes were used instead of stirrups respectively. The recorded first crack load noticed was 31.1 KN and 33.6 KN for B04 and B05 respectively. This showed an enhancement of about 36.4% and 47.4% respectively.

For specimen, B06 & B07 the recorded first crack load noticed was 32.2 KN and 46.3 KN for B06 and B07 respectively. This showed an enhancement of about 41.2 % and 103.1 % respectively, showing high enhancement in cracks.

Generally, the cracks for all tested beams started at the later stage of loading and started to

increase in number and length till failure, indicating better confinement and better serviceability. However, for different types of innovative composite, the ultimate strength

increased and the cracks slightly increased in length and width to a different extent. As shown in Figs. 7 to Fig. 10 and Table 5.



Fig. 7. Crack Pattern of Control Beam B01



a)



b)

Fig. 8. Crack Pattern of Group A, a) Beam B02; b) Beam B03.



a)



b)

Fig. 9. Crack Pattern of Group B, a) Beam B04; b) Beam B05.

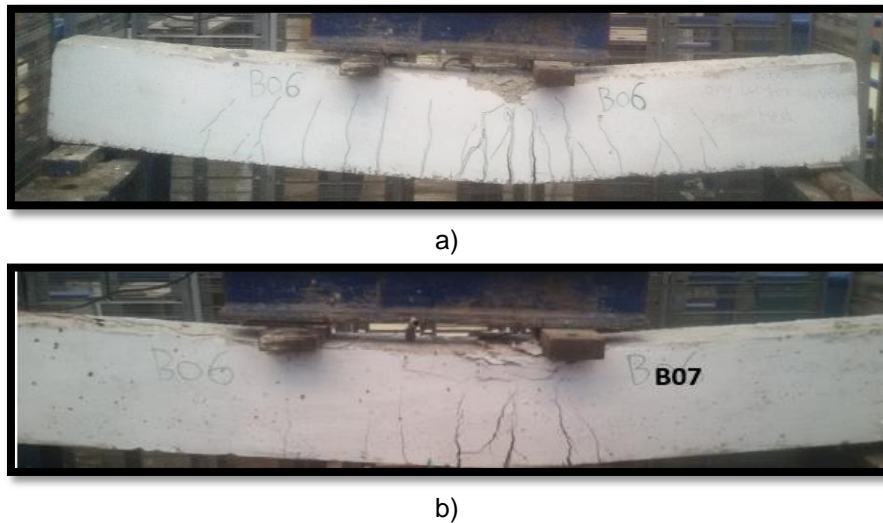


Fig. 10. Crack Pattern of Group C, a) Beam B06; b) Beam B07

3.6 Theoretical Calculation of Ultimate Flexural Load

The following assumptions are made in calculating the ultimate moment capacity of the beam.

- The strain in reinforcement and concrete is directly proportional to the distance from the neutral axis.
- The plane sections before loading remain plane and after loading.
- There is no relative slip between ferrocement laminate and the concrete.
- Failure occurs when the maximum compressive strain in the form's beam matrix and the concrete core reaches 0.0035.
- At ultimate load, the tensile contribution of the beam matrix and the concrete core is neglected and the compressive contribution is represented by a rectangular stress block of depth (a) equals 0.8dn and stress of 0.67fcu.
- The maximum compressive strain in concrete is 0.0035 in bending.
- The tensile strength of concrete is neglected.
- The mesh reinforcement in ferrocement laminate has a linear elastic stress-strain relationship to failure.
- Shear deformation is small.

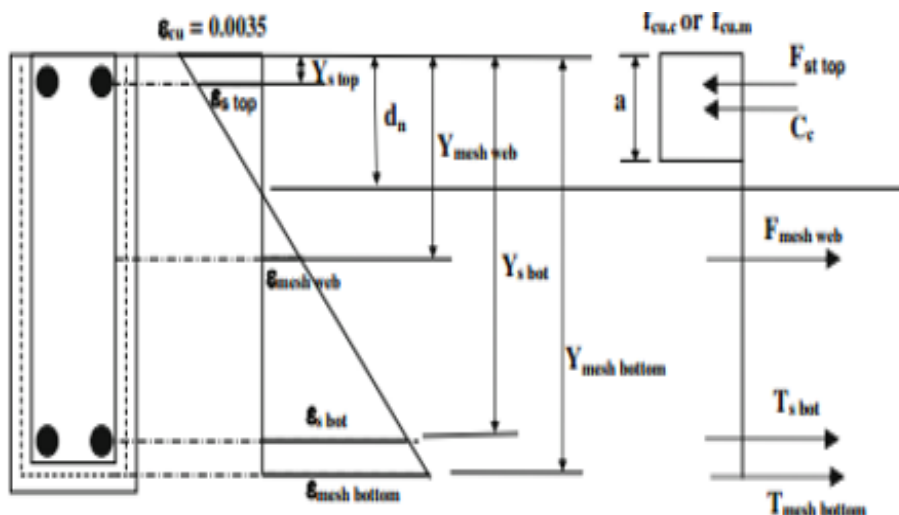


Fig. 11. Theoretical strain and Stress distribution and internal forces on the cross-section

$$(F_s.top + F_{mesh.web} + T_s.bot + T_{mesh.bot} - C_c) = 0 \quad (1)$$

The internal forces C_c , $F_s.top$, $F_{mesh.web}$, $T_s.bot$, and $T_{mesh.bot}$ are shown in Fig.11 and are given by:

- $C_c = ab f_{cu.c} \quad (2)$

- $F_s.top = \sigma_s.top A_s.top \quad (3)$

- $F_{mesh.web} = \sigma_{mesh.web} (2A_{mesh.web}) \quad (4)$

- $T_s.bot = \sigma_s.bot A_s.bot \quad (5)$

- $T_{mesh.bot} = \sigma_{mesh.bot} A_{mesh.bot} \quad (6)$

- $\sigma_s.bot = \epsilon_s.bot \leq F_{ys} \quad (\text{if } \epsilon_s.bot \leq \epsilon_{ys}) \quad (7)$

- $\sigma_s.bot = F_{ys} + E_{st} (\epsilon_s.bot - \epsilon_{ys}) \leq F_{us} \quad (\text{if } \epsilon_s.bot > \epsilon_{ys}) \quad (8)$

- $\sigma_s.top = \epsilon_s.top \leq F_{ys} \quad (\text{if } \epsilon_s.top \leq \epsilon_{ys}) \quad (9)$

- $\sigma_s.top = F_{ys} + E_{st} (\epsilon_s.top - \epsilon_{ys}) \leq F_{us} \quad (\text{if } \epsilon_s.top > \epsilon_{ys}) \quad (10)$

- $\sigma_{mesh.web} = \epsilon_{mesh.web} \leq F_{ym} \quad (11)$

- $\sigma_{mesh.bot} = \epsilon_{mesh.bot} \leq F_{ym} \quad (12)$

The strain at the top steel bars, bottom steel bars, web steel meshes, and bottom steel meshes could be obtained from the geometry of the strain distribution shown in Fig.11. $\sigma_s.top$ and $\epsilon_{mesh.web}$ could be tension (positive sign) or compression (negative sign) depending on the location of the neutral axis. The location of the neutral axis (X) is determined by applying trial and error method until Eq. (1) is satisfied. The calculation was performed on the computer using the Microsoft EXCEL sheet. Once the location of the neutral axis is determined and the internal forces are determined, the ultimate moment on the section (M_u) can be calculated by taking the moment about the point of application of the compression force as follows:

$$M_u = T_s.bot Y_s.bot + F_s.top Y_s.top + F_{mesh.web} Y_{mesh.web} + F_{mesh.bot} Y_{mesh.bot} \quad (13)$$

Accordingly, for simply supported beam subjected to central concentrated load, the ultimate load (P_u) is obtained from the following formula:

$$M_u = P_u * L/4 \quad (14)$$

3.7 List of Symbols

As.bot : Area of the steel bars at bottom of the beam.

As.top : Area of the steel bars at top of the beam (if they exist).

A_{mesh.bot} : Area of the steel meshes in the beam layer under the core.

A_{mesh.web} : The cross sectional area of the web mesh reinforcement in the vertical direction within a length equal to (d)

a : Depth of the compression block

b : Total width of the beam

C_c : The compressive force on the concrete block

d : The depth of the beam

dn : Neutral axis depth from the top of the specimen

E_s : Modulus of elasticity of the steel

F_{mesh.web} : The force on the mesh reinforcement in the two faces of the beam which could be positive or negative depending on the location of the neutral axis.

F_{s.top} : The force on the top reinforcement which could be positive or negative depending on the location of the neutral axis.

F_{ys}, F_{ym} : Yield stress or proof stress of the reinforcing steel bars and steel mesh

f_{cu.c} : Compressive strength of the concrete.

M_u : Ultimate moment of the beam

Pu : Ultimate load for flexural failure
Tmesh.bot : The tensile force on the steel mesh at the bottom of the beam
Ts.bot : The tension force on the bottom steel
ys.bot : Distance between the bottom steel bars and the compressive force (*Cc*)
ys.top : Distance between the top steel bars and the compressive force (*Cc*)
ymesh.web : Distance between the center of the web steel mesh and the compressive force (*Cc*)
ymesh.bot : Distance between the bottom steel meshes and the compressive force (*Cc*)
Esth : Strain-hardening modulus of the steel
Eys : Yield strain of the reinforcing steel bars
Emesh.web, σ mesh.web : Strain and stress at the level of mesh reinforcement at the sides of the beam
Emesh.bot, σ mesh.bot : Strain and stress at the level of mesh reinforcement at the bottom of the beam
Es.bot, σ s.bot : Strain and stress at the level of bottom steel bars
Es.top, σ s.top : Strain and stress at the level of top steel bars.

Table 6. Theoretical First Crack and Ultimate loads and Comparison with Experimental Results

Number	Distance to neutral axis from top of beam (mm)	Theoretical Moment (<i>Mu.theor</i>) (KN.M)	Theoretical load (<i>Pu.theor</i>) (kN)	Tested ultimate load <i>Pu</i> (kN)	<i>Pu.exp/Pu.theor</i>
B01	8.25	23.98	73.78	64	0.87
B02	34.70	29.42	90.54	68.5	0.76
B03	61.16	40.76	125.40	85.6	0.68
B04	35.59	29.84	91.81	64.3	0.70
B05	62.92	41.44	127.25	71.1	0.56
B06	70.11	44.11	135.73	88.5	0.65
B07	131.97	60.71	186.79	101.5	0.54

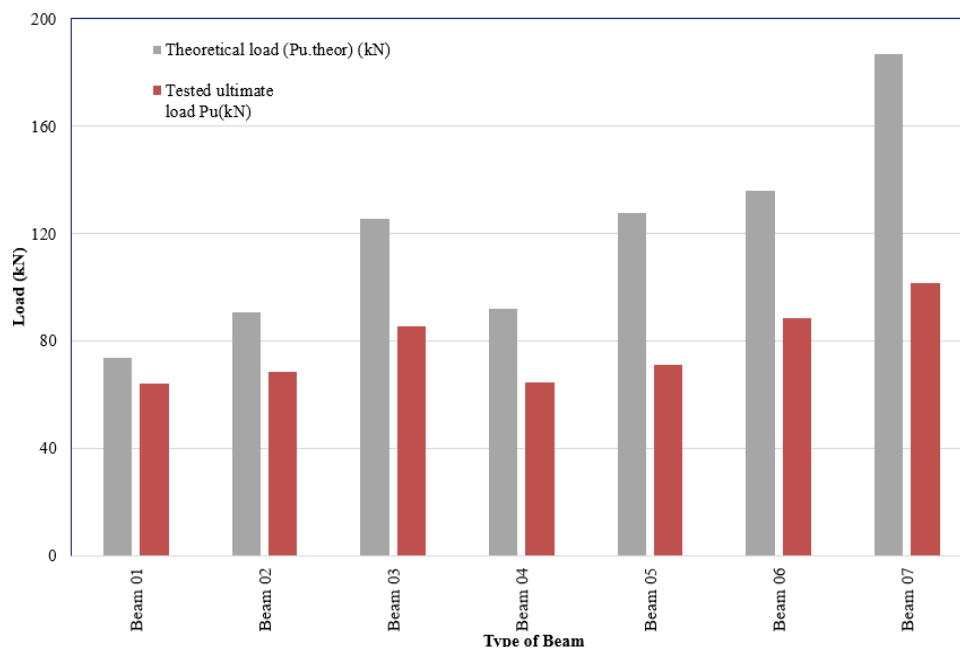


Fig. 12. Theoretical strain and Stress distribution and internal forces on the cross section

4. CONCLUSION

Based on the results and observations of the experimental study presented in this thesis and considering the relatively high variability and the statistical pattern of data, the following conclusions can be drawn:

- 1- Welded, expanded and woven wire meshes exhibited features over normal reinforcement with reinforcing steel, especially in rectangular beams such that, it has normal strength, easy to handling, cut, shaped and also has light weight.
- 2- The test results show that the woven wire mesh exhibited a higher ultimate load than conventionally reinforced control beams by about 39.1%.
- 3- Woven wire mesh has high effect in increasing load capacity, deflection, the flexural stresses and crack propagation.
- 4- Experimental results reveal that increasing the volume fraction of steel reinforcement contributed to a slightly higher ultimate load and higher energy absorption.
- 5- Therefore increasing volume fraction percentage has a dominant effect on delaying occurrence of the developed cracks with high protection against corrosion and high strength gain compared with those with metallic reinforcement.

COMPETING INTERESTS

Authors have declared that no competing interests exist.

REFERENCES

1. Mansur MN, Paramasivam P. Ferrocement Short Columns Under Axial and Eccentric Compression. *ACI structural Journal*. 1990;84(5):523.
2. Khan S. Strengthening of RC Beams IN Flexure Using Ferrocement. *IJST, Transactions of Civil Engineering, Proceedings*. 2013;37(C+):353-365.
3. Rashid H. Experimental and Numerical Analysis of Shear Deficient RC Beam Retrofitted With Ferrocement. 3rd International Conference on Civil Engineering for Sustainable Development. 2016;809-815.
4. Aqeel H. Chkheiwier Shear Behavior of Slender Ferrocement Box Beams," *Muthanna Journal for Engineering and Technology (MJET)* 2013.
5. Hazem R. Non-metallic Reinforcement for the U-shaped ferro-cement forms instead of the conventional steel mesh, *Deutsches Zentrum für Entwicklungs technologien*; 2009. Retrieved on February 20.
6. Abdel Tawab, Alaa. Development of permanent formwork for beams using ferro-cement laminates, P.H.D. Thesis, submitted to Menoufia University, Egypt; 2006.
7. Nagan S. Behaviour of Geopolymer Ferrocement Slabs Subjected to Impact," *IJST, Transactions of Civil Engineering*. 2014;38(C1+):223-233.
8. Abdel Tawab A. Use of permanent ferrocement forms for concrete beam construction. *Materials and Structures*; 2012.
9. Muna K. Self-Compacting Concrete: Design, Properties and Simulation of The Flow Characteristics in The L-Box. Doctor of Philosophy, Structural Department, Cardiff University, UK; 2016.
10. Fahmy, Yousry BI, Shaheen Ezzat H, Ahmed Mahdy Abdelnaby, Mohamed N, Abou Zeid. Applying the Ferro-cement Concept in Construction of Concrete Beams Incorporating Reinforced Mortar Permanent Forms. *International Journal of Concrete Structures and Materials*; 2013. Accepted November 27, 2013
11. ACI Committee 237. Self-consolidating concrete. ACI 237R-07, ACI Committee 237 Report, American Concrete Institute, Farmington Hills, Michigan. 2007;32.
12. Hassan AAA, Hossain KMA, Lachemi M. Structural assessment of corroded self-consolidating concrete beams. *Engineering Structures*. 2010;32:874-885.
13. Lachemi M, Hassain KMA, Lambros V, Nkinamubanzi PC, Bouzoubaa N. Self-compacting concrete in incorporating new viscosity modifying admixtures," *Cement and Concrete Research*. 2005;24:917-926.

14. Hassan SA. Behavior of reinforced concrete deep beams using self compacting concrete. PhD Thesis, University of Baghdad, Civil Department, Baghdad, Iraq. 2012;164.
15. Mahmoud KSH. Experimental study of the shear behavior of self compacted concrete T-beams, Journal of Engineering and Development, 2012; 16(1).

© 2021 Erfan et al.; This is an Open Access article distributed under the terms of the Creative Commons Attribution License (<http://creativecommons.org/licenses/by/4.0>), which permits unrestricted use, distribution, and reproduction in any medium, provided the original work is properly cited.

Peer-review history:

The peer review history for this paper can be accessed here:
<https://www.sdiarticle4.com/review-history/73935>